



Development of Predictive Thermodynamic Model for Liquefaction of Natural Gas Using the C3-Mr Refrigeration Process

Dagde, Kenneth, K., Okonkwo, Onochie, C.

Department of Chemical/ Petrochemical Engineering,
Rivers State University of Science and Technology, Port Harcourt, Nigeria

ABSTRACT

This paper presents a propane precooled mixed refrigerant (C3-MR) liquefaction plant with 4 pressure levels of propane cooling operational in Nigeria and demonstrates the procedure for developing a thermodynamic model that predicts the liquefied natural gas (LNG) production rate. The model prediction was validated with plant data with a maximum deviation of 3%. The thermodynamic efficiency of the natural gas liquefaction plant was estimated to be 45.1%. Simulations reveals that LNG production rate for the C3-MR plant depends on cooling water supply temperature (1 °C rise results to 92 tonnes per day of LNG loss), thermodynamic efficiency of the overall liquefaction process (1% drop results to 215 tonnes per day of LNG loss), LNG outlet temperature (1 °C decrease results to 108 tonnes per day of LNG loss), LNG production to feed gas supply ratio (1% rise results to 37 tonnes per day rise in LNG), thermal efficiency of gas turbine drivers (1% drop results to 277 tonnes per day of LNG loss), ambient air temperature (1 °C drop results to 67 tonnes per day of LNG increase) and feed gas supply pressure.

Keywords: natural gas, liquefaction, exergy, modeling, coefficient of performance, thermodynamic efficiency.

1. INTRODUCTION

The demand for natural gas is increasing rapidly to meet the accelerating increase in the worlds energy demand because natural gas is a more environmentally friendly and economical source of energy than other fossil fuels despite the fact that significant proportion of the worlds natural gas reserve is termed stranded gas. The drive to monetize large stranded gas reserves and put out the flares associated with crude oil production has led to the developments in Liquefied Natural Gas (LNG) technology (Finn et al, 1999).

The liquefaction of natural gas serves to reduce natural gas volume for economic transportation since LNG takes about 1/600th the volume of natural gas. Liquefaction of natural gas is energy intensive and is achieved by cooling natural gas below -160 °C. The basic principles for cooling and liquefying natural gas using refrigerants involves matching as closely as possible the cooling/heating curves of the process gas and the refrigerant resulting in a more efficient thermodynamic process. The natural gas liquefaction plant technology is currently dominated by the propane precooled mixed refrigerant cycle (C3-MR) licensed by Air Products and Chemicals Inc (APCI) (Finnet al., 1999, Bosma and Nagelwort, 2009).

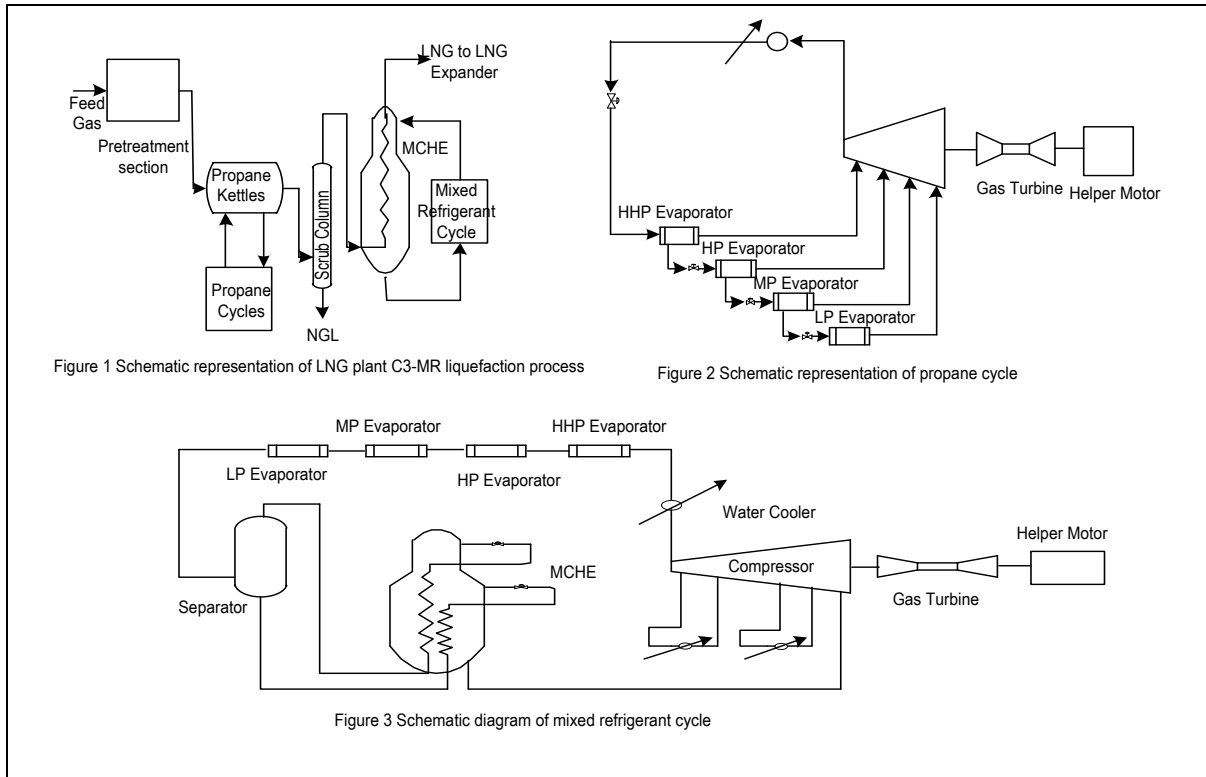
The plant considered in this study is a major LNG facility in Nigeria whose liquefaction process is based on the C3-MR cycle. In this process, which is illustrated in Fig. 1,

natural gas is cleaned and dried in a pretreatment section for the removal of CO₂, H₂O and Hg. The pretreated gas is then cooled in propane kettles to about -35 °C resulting in condensation of natural gas liquids (NGL) which is separated from the gas in the scrub column. The remaining gas after NGL extraction is liquefied and subcooled to about -161°C in the main cryogenic heat exchanger (MCHE) by exchanging heat with the evaporating mixed refrigerant. The LNG is then sent through an LNG expander to the LNG storage tank. The two refrigeration cycles present in the C3-MR process is the propane cycle, illustrated in Fig. 2, and the mixed refrigerant cycle, illustrated in Fig. 3. The propane cycle precools the natural gas and partially condenses the mixed refrigerant in the propane kettles and the mixed refrigerant cycle provides the required cooling in the MCHE. Power is delivered to the cycles by the gas turbines and helper motors (Brandt and Wesorick, 1994, Bosma and Nagelwort, 2009).

Tastaronis and Morosuk (2010) analyzed a three cascade system for the liquefaction of natural gas using conventional and advanced exergy analysis which revealed the potential for improving the thermodynamic efficiency of components and the overall system as well as the interactions among components and their effect on the exergy destruction within each component. Their study demonstrated some capabilities associated with advanced exergy analysis. Mafi *et al.* (2009) provided an exergy analysis for multicascade low temperature refrigeration systems with propylene and ethylene as

refrigerant used in olefin plant. The exergetic efficiency of the multistage cascade process was calculated to be 30.88%. The paper also proposed the replacement of the ethylene circuit with a mixed refrigerant circuit which showed improved exergetic efficiency of 34.04% due to closer temperature of approach in the heat exchangers. Ravavarapu *et al.* (1996) performed a comprehensive thermodynamic analysis of the propane precooled mixed refrigerant (C3-MR) process with 3 pressure levels of propane cooling. The results showed that the propane and

mixed refrigerant cycle operated at 34.3% and 58.3% thermodynamic efficiency respectively with an overall efficiency of 40.6%. Konoglu (2002) also provided a comprehensive thermodynamic analysis of a multistage cascade refrigeration cycle used in natural gas liquefaction. The exergetic efficiency was determined to be 38.5%. Remeliej and Hoadley (2007) concentrated on the duty curve to analyse the efficiency of heat exchange trains of LNG plant.



Previous works related to the present research have been based on rigorous thermodynamic analysis and process simulation using thermodynamic models constructed in process simulation software such as Aspen HYSIS, PRO II and Unisim. These studies were limited to the calculation of the thermodynamic efficiency of different natural gas liquefaction processes and investigation of different approaches to improve thermodynamic efficiency within the process (Ibrahim *et al.*, 2011, Khalipour and Karimi, 2012, Rodgers *et al.* 2012, Span and Dauber, 2012). The main objective of this research paper is to demonstrate the applicability of a simple thermodynamic model, which does not involve constructing equipment models in process simulation software, to quickly predict the LNG production rate of a functional industrial LNG plant. This is achieved by obtaining plant process data from a major LNG facility and validating the model prediction to actual LNG production rates of the plant. In this paper also, a model for the maximum expected LNG production rate when all

the power available to the process is utilized is developed. This paper also investigates the sensitivity analysis of LNG production rate of the plant.

2. MODEL DEVELOPMENT

Figure 4 shows the simplified hypothetical flow scheme of a typical natural gas liquefaction process. The simplified typical natural gas liquefaction plant consists of a cooling water condenser, expander, main heat exchanger, compressor and a gas turbine driver. The refrigerant is compressed in the compressor to a high pressure at which it is condensed at the cooling water temperature in the condenser. The pressure of the refrigerant is then let down in an expander or flash valve to a low pressure. Its temperature also decreases as a result of reduction in pressure. The refrigerant is sent through the main heat exchangers where it cools and liquefies the natural gas to produce LNG. A portion of the

feed gas (fuel gas) is used to run the gas turbine which drives the compressor.

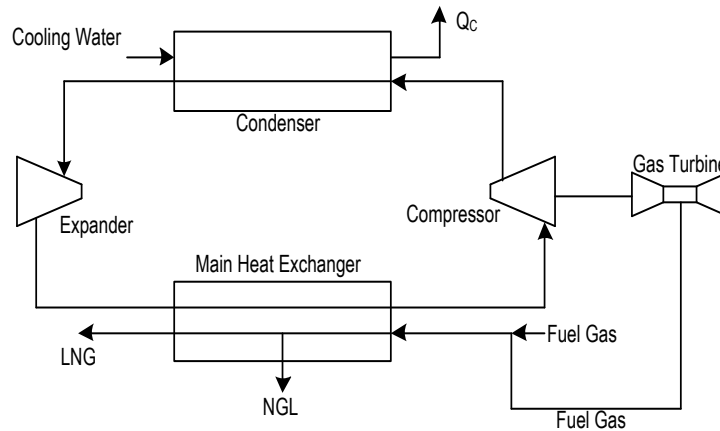


Figure4. Simplified hypothetical flow scheme of a typical natural gas liquefaction process

The exergy analysis of the liquefaction process is based on the following assumptions:

- A. The Composition of feed gas stream is the same as the composition of the LNG stream.
- B. No NGL extraction occurs as the natural gas is liquefied.
- C. LNG production rate is the same as the feed gas supply to the main heat exchanger
- D. The main heat exchanger is adiabatic.

The reversible work (W_{revin}) required to liquefy natural gas based on the above assumptions, is given by the exergy (X) change between the inlet and outlet states as

$$W_{revin} = X_2 - X_1 = h_2 - h_1 - T_o(S_2 - S_1) \quad (1)$$

where subscripts 1 and 2 represent the inlet state of natural gas and outlet state of LNG respectively, h is specific enthalpy, S is specific entropy and T_o is cooling water (dead state) temperature.

The refrigeration duty (Q) based on the above assumptions, is given by

$$Q = h_1 - h_2 \quad (2)$$

where, h_1 and h_2 are the specific enthalpy at inlet and outlet states respectively.

The reversible Coefficient of Performance (COP_{rev}) which is the ratio of the refrigeration duty to the reversible work required is obtained as

$$COP_{rev} = \frac{1}{T_o \left(\frac{S_2 - S_1}{h_2 - h_1} \right) - 1} \quad (3)$$

The Coefficient of Performance (COP) of actual natural gas liquefaction processes is

$$COP = \frac{\eta_R}{T_o \left(\frac{S_2 - S_1}{h_2 - h_1} \right) - 1} \quad (4)$$

where η_R is the thermodynamic or exergetic efficiency.

Equation 4 is the model for the coefficient of performance of actual natural gas liquefaction processes.

Considering Figure 4, based on the assumption that the main heat exchangers are adiabatic and that the feed gas and LNG composition are constant. The refrigeration duty for production of LNG is

$$Q = \dot{m}_{NG}(h_{in} - h_{T1}) + \dot{m}_{LNG}(h_{T2} - h_{out}) \quad (5)$$

where the subscripts in and out represents the inlet and outlet states for natural gas and LNG respectively, T_1 and T_2 represents the NGL extraction conditions for natural gas and LNG respectively, \dot{m}_{NG} and \dot{m}_{LNG} is the feed gas supply rate and LNG production rate respectively. Neglecting the expander work output since it is negligible when compared to the compressor work input which is

provided by the gas turbine driver, the network input ($W_{net\ in}$) to the liquefaction process is given by

$$W_{net\ in} = W_{comp} = W_{turb} \quad (6)$$

Where, W_{comp} and W_{turb} are work required by the compressors and work delivered by the gas turbines respectively.

The COP of the actual liquefaction process is given by

$$COP = \frac{\dot{m}_{NG} (h_{in} - h_{T1}) + \dot{m}_{NG} (h_{T2} - h_{out})}{W_{comp}} \quad (7)$$

$$\dot{m}_{LNG} = \frac{W_{comp}}{\left(\frac{1}{\frac{\dot{m}_{LNG}}{\dot{m}_{NG}}} \right) (h_{in} - h_{T1}) + (h_{T2} - h_{out})} \left[\frac{\eta_R}{T_o \left(\frac{S_2 - S_1}{h_2 - h_1} \right) - 1} \right] \quad (8)$$

The ratio of LNG produced to natural gas feed $\left(\frac{\dot{m}_{LNG}}{\dot{m}_{NG}} \right)$ depends on the scrub column performance and composition of feed gas and LNG. This ratio can be determined from individual LNG liquefaction plants. Equation 9 describes the model equation for LNG production rate and can be modified by substitution of appropriate parameters to tailor it for specific LNG plants.

The compressor work input (W_{comp}) is given by;

$$W_{comp} = W_{PR} + W_{MR} + HM_{PR} + HM_{MR} \quad (10)$$

where W_{PR} , W_{MR} , HM_{PR} and HM_{MR} are the work input from the propane compressor turbine, mixed refrigerant compressor turbine, power delivered by the propane

Rearranging equation 7 yields

$$\dot{m}_{LNG} = \frac{W_{comp} COP}{\left(\frac{1}{\frac{\dot{m}_{LNG}}{\dot{m}_{NG}}} \right) (h_{in} - h_{T1}) + (h_{T2} - h_{out})} \quad (8)$$

Combining equation 8 and equation 4 yields

compressor helper motor and mixed refrigerant compressor helper motor.

But,

$$W_{PR} = \dot{m}_{fg} h_c \eta_{PR} \quad (11)$$

$$W_{MR} = \dot{m}_{fg} h_c \eta_{MR} \quad (12)$$

where \dot{m}_{fg} , h_c , η_{PR} and η_{MR} are the fuel gas flow rate to the gas turbines, specific heat of combustion of fuel gas, thermal efficiency of propane cycle gas turbine and thermal efficiency of mixed refrigerant cycle gas turbine.

Substituting equation 12, 11 and 10 into equation 9 yields

$$\dot{m}_{LNG} = \frac{\dot{m}_{fg} h_c \eta_{PR} + \dot{m}_{fg} h_c \eta_{MR} + HM_{PR} + HM_{MR}}{\left(\frac{1}{\frac{\dot{m}_{LNG}}{\dot{m}_{NG}}} \right) (h_m - h_{T1}) + h_{T2} - h_{out}} \left[\frac{\eta_R}{T_o \left(\frac{S_2 - S_1}{h_2 - h_1} \right) - 1} \right] \quad (13)$$

Equation 13 describes the model equation for LNG production rate for the LNG facility.

The maximum power delivered by a gas turbine is a function of the ambient (T_a) and is given by

$$\text{Turbine Power output} = A(BT_a + C) \quad (14)$$

$$\dot{m}_{LNG,max} =$$

$$\frac{38300(-0.00708 T_a + 1.1062) + 82700(-0.00693 T_a + 1.1040) + 2 \times 8700}{\left(\frac{1}{\frac{\dot{m}_{LNG}}{\dot{m}_{NG}}} \right) (h_m - h_{T1}) + h_{T2} - h_{out}} \left[\frac{\eta_R}{T_o \left(\frac{S_2 - S_1}{h_2 - h_1} \right) - 1} \right] \quad (15)$$

Equation 15 describes the model equation for the maximum expected LNG production rate from the LNG facility when the turbines and helper motors are operated at full capacity.

3. OPERATING DATA/SOLUTION TECHNIQUES

The data required includes the composition of feed gas, LNG and fuel gas as shown in Table 1. Other operating data needed includes the feed gas temperature and pressure, NGL extraction temperature and pressure, LNG outlet temperature and pressure, fuel gas flow rate to PR and MR turbines, PR and MR turbine inlet air temperature (Ambient air temperature), cooling water temperature, PR Helper motor power and MR helper motor power. These data were obtained from the plant during its operation. The thermal efficiency of the PR turbine and MR turbine were estimated from data obtained during periods of maximum LNG production when both turbines are operated at full capacity.

In other to obtain the solution to equation 13 and 15, ASPEN HYSYS VERSION 3.2 simulation software on the basis of Peng-Robinson equation of state was used to obtain the required thermodynamic properties (enthalpy, entropy and heat of combustion) by inputting the composition, temperature and pressure required. Equations 13 and 15 are simple algebraic equations and their solutions were obtained using Microsoft excel spreadsheet.

where A is ISO base load rating of the turbine, B and C are constants and T_a is ambient (gas turbine inlet) temperature. A, B and C were obtained from the performance curves of the gas turbines. B and C were estimated by fitting the gas turbine percent design output against inlet air temperature graph with a straight line.

The maximum expected LNG production from the plant is given by

Table 1 Composition of feed gas, LNG and fuel gas (Nigeria LNG, 2000)

Component	Composition (% mol fraction)		
	Feed gas	LNG	Fuel gas
Nitrogen (N ₂)	0.116	0.118	0.0887
Methane (C ₁)	90.736	91.526	93.7021
Ethane (C ₂)	4.487	4.4	4.1059
Propane (C ₃)	2.602	2.482	1.4715
Iso-Butane (iC ₄)	0.553	0.579	0.3061
Butane (C ₄)	0.835	0.883	0.3147
Iso-Pentane (iC ₅)	0.254	0.009	0.0062
Pentane (C ₅)	0.183	0.002	0.0036
Hexane (C ₆)	0.145	0	0.0011
Heptane(C ₇)	0.078	0	0
Octane (C ₈)	0.014	0	0
Nonane (C ₉)	0.002	0	0
Decane (C ₁₀)	0.001	0	0

4. RESULTS AND DISCUSSION

Table 5 shows the comparison between model predictions, maximum model predictions and actual plant data for the LNG production (Tons/Day). The model prediction and maximum model prediction was obtained from equations 13 and 14 respectively. The maximum % deviation of the model predictions from plant data is 3% which is about 300Tons/Day of LNG. Most of the model predictions fall within 2% deviation from plant data. The deviation of the model prediction from the plant data is due to the assumptions (1 – 4) made when calculating the COP of the liquefaction process from exergy analysis and the assumption that the feed gas composition and LNG

composition are constant for all data points. There is a difference between the LNG composition and feed gas composition and the LNG production rate and feed gas supply rate due to NGL extraction in the scrub column to remove heavies from the feed gas stream. During NGL extraction a significant amount of methane is lost in the NGL stream. Although the main cryogenic heat exchanger and propane kettles and their associated piping are insulated, there is usually some heat leak into the process from the environment. Some slight deviation may also occur from the use of the Peng-Robinson equation of state to calculate the thermodynamic properties of enthalpy and entropy and instrument error in obtaining data from the plant.

Table5: Comparison between model prediction, maximum model prediction and plant data

Plant LNG Production (T/D)	Model Prediction (T/D)	%Deviation	Maximum model Prediction(T/D)	% Plant Operating Efficiency
9878	9690	-1.90	10382	95.1
9830	9643	-1.91	10231	96.1
9804	9862	0.60	10349	94.7
9796	9773	-0.23	10474	93.5
9781	9730	-0.53	10241	95.5
9757	9829	0.74	10131	96.3
9744	9655	-0.91	10235	95.2
9733	9514	-2.25	10040	96.9
9713	9700	-0.13	10063	96.5
9690	9716	0.27	10186	95.1
9667	9730	0.65	9951	97.1
9639	9640	0.01	10270	93.9
9620	9490	-1.35	10104	95.2
9595	9472	-1.28	9902	96.9
9563	9291	-2.85	9876	96.8
9552	9504	-0.50	9911	96.4
9534	9537	0.03	9921	96.1
9510	9605	1.00	9906	96.0
9490	9479	-0.12	9817	96.7
9473	9513	0.42	9821	96.5
9465	9388	-0.82	9695	97.6
9443	9504	0.65	10078	93.7
9427	9443	0.18	9697	97.2
9413	9424	0.11	9684	97.2
9400	9443	0.45	9641	97.5
9385	9672	3.06	9930	94.5
9365	9404	0.42	9666	96.9
9355	9430	0.80	9753	95.9
9336	9432	1.03	9743	95.8
9307	9455	1.59	9700	95.9
Maximum % Deviation			3.06%	
Average %Plant Operating Efficiency			95.40%	

Plant Thermodynamic Efficiency	45.10%	
--------------------------------	--------	--

The overall thermodynamic efficiency of the C3-MR liquefaction process with 4 pressure levels of propane cooling was estimated to be 45.1%. Ravavarapu *et al.* (1996) overall thermodynamic efficiency for C3-MR liquefaction process with 3 pressure levels of propane cooling was 40.6%. This shows that the addition of an extra pressure level of propane cooling increased the thermodynamic efficiency of the liquefaction process as expected by about 11% due to lower temperature of approach in the propane kettles.

Figure 5 shows the trend of plant LNG production rate (plant data), model prediction and maximum model prediction. The maximum model prediction is always above the plant data and it follows the trend of the plant data with an average deviation of about 500T/D LNG as shown in Figure 5. This shows the window available to optimize LNG production and shows that the plant is operating at about 95% of theoretical maximum.

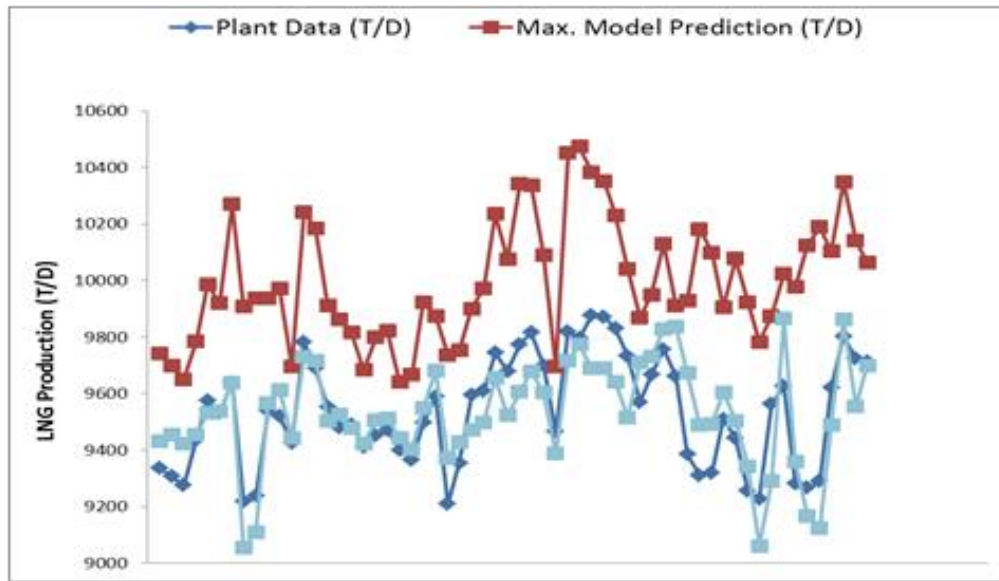


Figure 5. Trend of Plant data, Maximum model prediction and model prediction for LNG production rate

This deviation may be due to transmission losses from the turbines to the compressors and some excess capacity in the propane cycle due to the fact that the MR cycle is limiting.

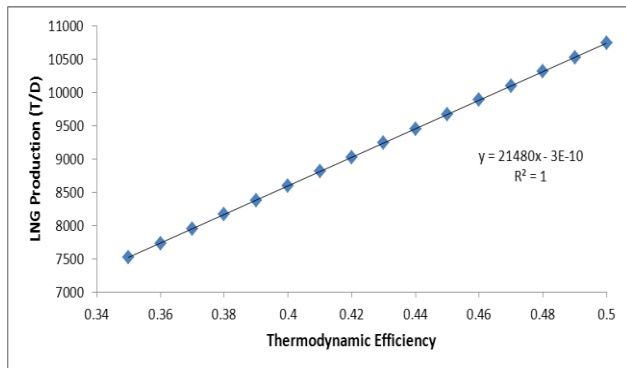


Figure 6. Graph of LNG Production against thermodynamic efficiency

From the results, the model as described by equation 13 and 14 is accurate. Figure 6 shows the graph of LNG production against overall thermodynamic efficiency of the liquefaction process. The LNG production increases linearly with thermodynamic efficiency. A 1% increase in overall thermodynamic efficiency results in a 215T/D increase in LNG production. Various factors affects the overall thermodynamic efficiency of the liquefaction process and it includes the liquefaction plant configuration, the average temperature of approach in the heat exchangers, heat leak into the process and particularly for the C3-MR liquefaction process, the level in the propane kettles, MR composition, Heavy MR to Light MR ratio, the position of the propane and MR compressors recycle valves etc. For instance, if the MR composition is not optimized, the temperature of approach in the main cryogenic heat exchanger will be larger.

This generates more entropy in the heat transfer process reducing the thermodynamic efficiency of the process leading to lesser LNG production. As thermodynamic

efficiency of the process decreases, the COP of the liquefaction process decreases thereby resulting in lower LNG production for the same amount of power. This suggests that natural gas liquefaction processes with higher overall thermodynamic efficiencies produces more LNG.

Figure 7 shows the graph of LNG production against cooling water temperature. The LNG production rate decreases linearly as the cooling water temperature increases. A 1 °C increase in cooling water temperature results in a 92T/D decrease in LNG production. An increase in cooling water temperature decreases LNG production because the cooling water temperature determines the discharge pressure of the propane compressor.

An increase in cooling water temperature increases the discharge pressure of the propane compressor. This results in reduced flow of propane refrigerant, lower refrigeration capacity and therefore lower LNG production. Also as the cooling water temperature increases, the COP of the liquefaction process decreases, thereby resulting in lower LNG production for the same amount of power. This suggests that addition of corrosion inhibitors to the cooling water to minimize fouling of the cooling water exchangers and adequate maintenance (cleaning) of the cooling water heat exchangers to remove restrictions which reduce the cooling water flow rate in the heat exchangers causing higher cooling water return temperatures and therefore higher cooling water supply temperatures from the cooling tower would keep the LNG production rates at its maximum. Refrigeration of the cooling water is also an option to increase LNG production rates.

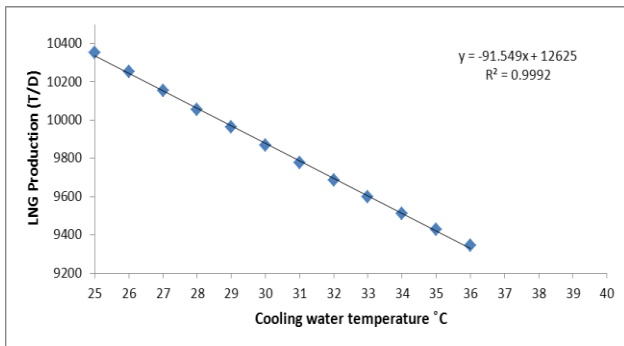


Figure 7. Graph of LNG production against cooling water Temperature

Figure 8 shows the graph of LNG production against the LNG outlet temperature. The LNG production rate decreases linearly with decreasing LNG outlet temperature. A 1 °C decrease in LNG outlet temperature results in a 108T/D decrease in LNG production. A decrease in LNG outlet temperature decreases the LNG

production rate because the refrigeration duty required to achieve a much lower temperature is increased.

Also as the LNG outlet temperature decreases, the change in exergy ($W_{rev in}$) increases leading to a decrease of the COP of the process thereby resulting in lower LNG production for the same amount of power. This suggests that cooling the LNG beyond its design temperature of -161 °C is not advantageous. It is important to note that higher LNG temperatures also results in LNG losses due to increased boil off gas production rates in the LNG storage tanks and during loading operations.

Figure 9 shows the graph of LNG production against LNG production to feed gas supply ratio. The LNG production rate increases linearly with LNG production to feed gas supply ratio. A 1% increase in LNG to feed gas ratio results in a 37T/D increase in LNG production. This ratio is determined mainly by the performance of the scrub column and NGL recovery. A scrub column which minimizes methane losses to the NGL stream has a better performance. As more methane is lost to the NGL stream, the LNG to feed gas ratio decreases. For deeper NGL recovery (LPG recovery), the scrub column temperature is reduced, more methane is lost to the NGL stream and the LNG becomes leaner.

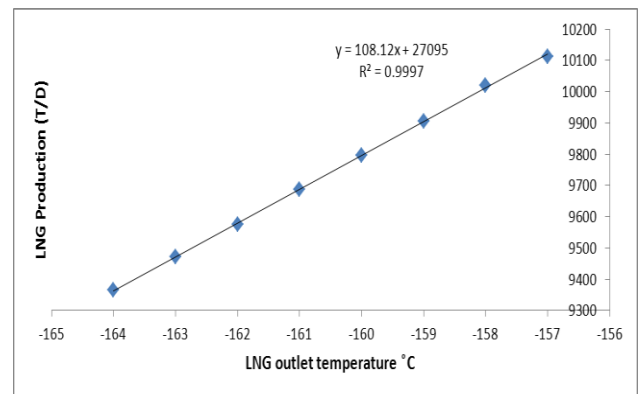


Figure 8 Graph of LNG production against LNG outlet temperature

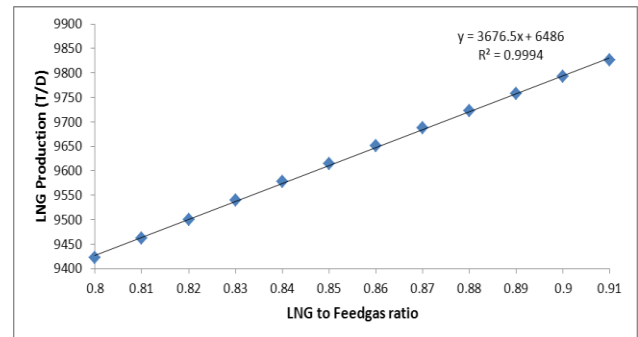


Figure 9. Graph of LNG production against LNG to feed

gas ratio

Therefore as NGL recovery increases, LNG to feed gas ratio decreases. As the LNG to feed gas ratio decreases, LNG production decreases due to the increased methane losses in the NGL stream as the power which is used to cool it to the NGL extraction temperature is lost. This suggests that as NGL or LPG recovery from the feed gas increases, the LNG production rate falls.

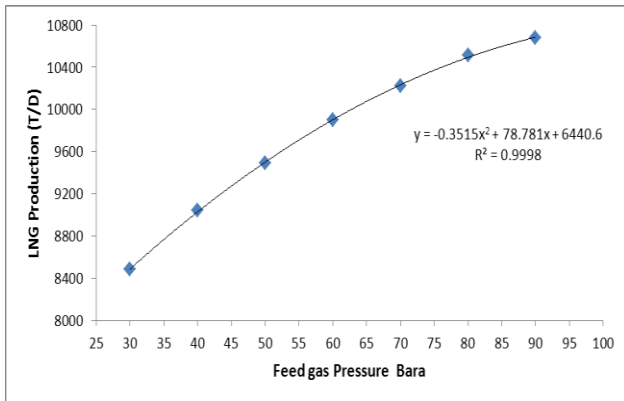


Figure10. Graph of LNG production against Feed gas Pressure

Figure 10 shows the graph of LNG production against feed gas supply pressure assuming a constant pressure drop of 15 bars in the entire process. The LNG production rate increases with feed gas pressure but at a reducing rate. An increase in feed gas pressure results in an increase in LNG production because at higher pressures the feed gas liquefies at higher temperatures (with smaller enthalpies of condensation) and lower refrigeration duty which is more efficient. The exergy change ($W_{rev in}$) decreases as feed gas pressure increases resulting to an increase in the COP of the process which leads to higher LNG production. This suggests that LNG plants designed for higher operating pressure produces more LNG.

Figure 11 shows the graph of LNG production against ambient air temperature. The LNG production decreases linearly as ambient air temperature increases. A 1 °C increase in ambient temperature results in a 67T/D decrease in LNG production. An increase in ambient temperature results to a decrease in LNG production because the gas turbine power output reduces with increase with ambient temperature. Gas turbines are constant volume machines and as such increases in ambient temperature, decreases the air density and therefore the mass flow rate of air intake by the turbine.

This results in lower fuel gas intake and lower power output from the gas turbine to drive the refrigerant compressors. This suggests that cooling of the gas turbine

inlet air temperature would result in higher LNG production rates.

Figure 12 shows the graph of LNG production against thermal efficiency of the gas turbine drivers. The LNG production rate decreases linearly as the thermal efficiency of the gas turbines decreases. A 1% decrease in thermal efficiency results in a 277T/D decrease in LNG production rate. As the gas turbine is being used, the gas turbine performance (thermal efficiency) degrades with time. This is due to compressor fouling, deposition on turbine blades and degradation of parts (changes in airfoil contour and surface finish, wear and corrosion). Higher efficiency gas turbine drivers deliver more LNG for the same amount of fuel gas. Decrease in gas turbine efficiency decreases LNG production because lesser power is obtained from the gas turbine to drive the refrigerant compressors. This suggests that adequate operation and maintenance schedule (water wash, inspection, replacement of degraded parts) of the gas turbine drivers would keep LNG production at maximum rates in the long term.

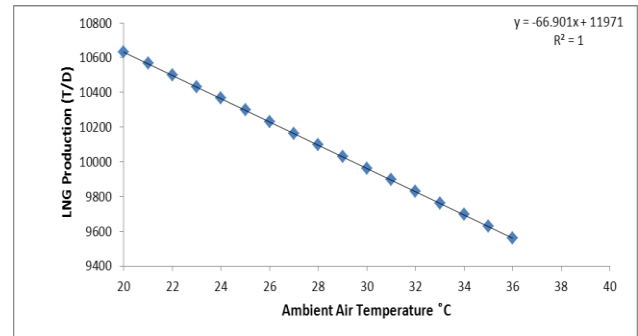


Figure 11. Graph of LNG production against ambient air temperature (Gas turbine inlet air temperature)

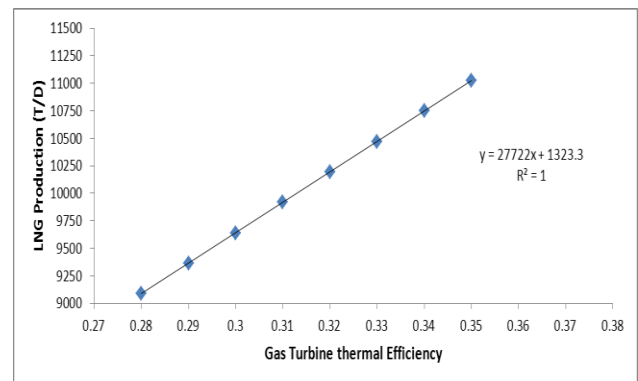


Figure 12 Graph of LNG productions against thermal efficiency of gas turbine

5. CONCLUSION

A thermodynamic model that predicts the LNG production rate of an LNG plant was developed. The model prediction was validated with plant data from an LNG plant operational in Nigeria. The thermodynamic efficiency of the natural gas liquefaction plant was estimated to be 45.1%. The plant was producing LNG at an average of 95% of the theoretical maximum. Simulations reveals that LNG production rate for the C3-MR plant operational in Nigeria depends on cooling water supply temperature (1 °C rise results to 92T/D LNG loss), thermodynamic efficiency of the overall liquefaction process (1% drop results to 215T/D LNG loss), LNG outlet temperature (1 °C decrease results to 108T/D LNG loss), LNG production to feed gas supply ratio (1% rise results to 37T/D rise in LNG), thermal efficiency of gas turbine drivers (1% drop results to 277T/D LNG loss), ambient air temperature (1 °C drop results to 67T/D LNG increase) and feed gas supply pressure.

This paper suggests that in other to keep LNG production in this LNG plant at its maximum, the LNG should not be cooled beyond the design temperature of -161 °C, there should be adequate maintenance and inspection of the gas turbines, cleaning of the cooling water heat exchangers and optimization of process parameters. This paper also suggests that refrigeration of cooling water and gas turbine inlet air are available options to increase LNG production for this LNG facility.

The model developed can be adapted to other LNG plants by substituting specific equations for compressor work input into the refrigeration cycle and substituting the LNG to feed gas ratio.

REFERENCES

- [1] Bosma, P., Nagelwort, R.K. Liquefaction Technology: Developments through History, Proceedings of the first Annual Gas Processing Symposium, Doha, Qatar: 1-13, (2009).
- [2] Brandt, D.E., Wesorick R.R. GE Gas Turbine Design Philosophy, GE Industrial & Power Systems Schenectady, NY, GER-3434D, (1994).
- [3] Finn, A. J., Johnson, G. L., Tomlinson, T. R. "Development in Natural Gas Processing"; Hydrocarbon Processing, (April): 78, (1999).
- [4] Ibrahim, T.K., Rahman, M.M., Abdalla, A.N. Improvement of Gas Turbine Performance based on Inlet Air Cooling Systems: A Technical Review, International Journal of Physical Sciences, 6(4): 620-627, (2011).
- [5] Khalilpour, R., Karimi, I. A. Evaluation of Utilization Alternatives for Standard Natural gas; Energy, **40**: 317-328, (2012).
- [6] Konoglu, M. Exergy Analysis of Multistage Cascade Refrigeration Cycle used for Natural Gas Liquefaction; International Journal of Energy Research, **26**: 763-774, (2000)
- [7] Mafi, M., Mousavi, S. M., Amidpour, M. Exergy Analysis of Multistage Cascade Low Temperature Refrigeration Systems used in Olefin Plants; International Journal of Refrigeration, **32**: 279-294, (2009).
- [8] Nigeria LNG Operating manual UNIT 1400 Liquefaction, (2000)
- [9] Ravavarapu, V. Oakley, J., H. and White, C., C. Thermodynamic Analysis of a Baseload LNG Plant; Proceeding of the Chemeca 96: Excellence in Chemical Engineering: 24th Australian and New Zealand Chemical Engineering Conference and Exhibition: 143-148, (1996).
- [10] Remeliej, C.W., Hoadley, A.F.A. "An Exergy analysis of Small-scale Liquefied Natural gas (LNG) Liquefaction Processes"; Energy, **31**: 2005-2019, (2006).
- [11] Rodgers, P., Mortazavi, A., Eveloy, V., Al-Hashimi, S., Hwang, Y., Radermacher, R. Enhancement of LNG Plant Propane Cycle through Waste Heat powered Absorption cooling, Applied Thermal Engineering, **48**: 41-53, (2012).
- [12] Span, R., Dauber, F. "Modelling Liquefied-Natural-Gas Processes using highly accurate Property Models", Applied Energy, **97**: 822-827. (2012)
- [13] Tsatsaronis, G., Morosuk, T. "Advanced Exergetic Analysis of a Refrigeration System for Liquefaction of Natural gas"; International Journal of Energy and Environmental Engineering, **1**, (Fall): 1-17, (2010).

NOMENCLATURES

- \dot{m}_{NG} = Feed gas (natural gas) supply rate (Kg/s)
- \dot{m}_{fg} = fuel gas flow rate (Kg/s)
- \dot{m}_{LNG} = LNG production rate (Kg/s)
- η_{MR} = Thermal efficiency of MR turbine
- η_{PR} = Thermal efficiency of PR turbine

η_R	=	Thermodynamic efficiency of overall liquefaction process
COP	=	Coefficient of Performance
COP _{rev}	=	Reversible Coefficient of Performance
H	=	Specific enthalpy (KJ/Kg)
h_c	=	Specific heat of combustion (KJ/Kg) of fuel gas
HM	=	Helper motor power (KW)
Q	=	Refrigeration duty (KW)
S	=	specific entropy (KJ/Kg K)
T_a	=	Ambient (Gas turbine inlet air) temperature ($^{\circ}$ C)
T_o ($^{\circ}$ C)	=	cooling water (dead state) Temperature
W	=	Work input (KW)
W_{comp}	=	Compressor work (KW)
$W_{net\ in}$	=	net work input (KW)
$W_{rev\ in}$	=	Reversible work (KJ/Kg)
W_{turb}	=	Turbine power (KW)
X	=	Specific exergy (KJ/Kg)

ABBREVIATIONS

C3-MR	=	Propane precooled mixed refrigerant liquefaction process
MR	=	Mixed refrigerant
LNG	=	Liquefied natural gas
NGL	=	Natural gas liquids
PR	=	Propane
MCH	=	Main cryogenic heat exchanger
APCI	=	Air Products and Chemicals Inc.